

$\pi^+ d \rightarrow \pi^+ pn$ reaction as a test of relativistic Faddeev theories: Vector analyzing power

W. Gyles, E. T. Boschitz, H. Garcilazo,* E. L. Mathie,[†] C. R. Ottermann, and G. R. Smith[‡]
*Kernforschungszentrum Karlsruhe, Institut für Kernphysik and Institut für Experimentelle Kernphysik der Universität Karlsruhe,
7500 Karlsruhe, Federal Republic of Germany*

S. Mango and J. A. Konter
Schweizerisches Institut für Nuklearforschung, 5234 Villigen, Switzerland

R. R. Johnson
TRIUMF, University of British Columbia, Vancouver, British Columbia, Canada V6T 2A3
(Received 30 July 1985)

The vector analyzing power, iT_{11} , has been measured for the $\pi^+ d \rightarrow \pi^+ pn$ reaction in a kinematically complete experiment. The dependence of iT_{11} on the momentum of the proton has been obtained for 35 pion-proton angle pairs at pion bombarding energies of 180, 228, and 294 MeV. The data are compared with a relativistic Faddeev calculation. The theoretical prediction that there is a single universal shape for iT_{11} , which is positive at low proton momenta and negative at large proton momenta, independent of the final pion and proton angles or of the incident pion energy is confirmed by the experiment.

I. INTRODUCTION

After the discovery of unexpected structure in spin-dependent nucleon-nucleon scattering above the pion threshold,¹ a wealth of polarization measurements in the πNN system has enriched the body of existing data and put conventional theories to a stringent test.²

In the πd elastic scattering reaction, measurements of the vector analyzing power iT_{11} (Ref. 3) and the tensor polarization t_{20} (Ref. 4) demonstrated the importance of the small πN partial waves for the theoretical input; in particular they have raised serious questions on the proper treatment of the P_{11} πN partial wave.⁵ This latter issue is not settled but it is already clear that reliable and extensive data on the tensor polarization t_{20} are needed to constrain the P_{11} πN input.⁶

In the $pp \rightarrow \pi^+ d$ reaction, the polarization observables A_{xz} , A_{y0} , and iT_{11} serve as another example. These observables are very sensitive to details of the theory and there are severe problems in simultaneously reproducing all of them over a large energy range.⁷ For a detailed discussion see Ref. 8. The particular significance of some polarization data in this reaction has been shown by a partial wave analysis by Bugg.⁹ Making use of the recent measurements of the vector analyzing power iT_{11} ,¹⁰ he was able to tightly constrain the previously undetermined amplitude a_3 ($NN P_1^3 \rightarrow \pi d$, $l=2$) in both magnitude and phase; thereby reducing the uncertainties of the other amplitudes as well.

Finally, polarization measurements have been carried out in the $NN \rightarrow \pi NN$ reaction channel. For the $pp \rightarrow \pi pn$ reaction the asymmetry A_y and the spin-spin correlation parameters A_{yy} and A_{zz} were studied at LAMPF (Refs. 11 and 12), and at TRIUMF.¹³ The in-

elastic cross sections in longitudinal spin states $\Delta\sigma_L^{\text{inel}}$ were measured at LAMPF (Ref. 14) and at SIN.¹⁵ From these measurements it appears that the current π -exchange models fail most dramatically for longitudinal spin states at energies around 800 MeV (Ref. 16). The serious discrepancies from Deck model calculations were considered suggestive for the existence of other mechanisms like the excitation of dibaryon resonances.^{16,17}

From this brief discussion it is obvious that polarization experiments are important for testing finer details of conventional theories describing the NN and πNN system, and may possibly shed some light on the still open question regarding the existence of dibaryon resonances. Measurements of spin dependent observables in the dominant πd channel, the πd breakup reaction, are therefore highly desirable, but so far nonexistent. For this reason we have begun to investigate the observable iT_{11} in a kinematically complete experiment over a large region of phase space. A sample of the first results at $T_\pi=228$ MeV has been reported recently.¹⁸ In this paper extensive data for many pairs of proton and pion angles at 180, 228, and 294 MeV incident pion energy are presented.

II. EXPERIMENTAL TECHNIQUE

The experiment was conducted at the $\pi M3$ area of the Swiss Institute for nuclear Research (SIN), with the same detection system as was described in the preceding paper. The vector analyzing power was determined by measuring the spin dependent breakup cross sections, σ^+ and σ^- , for the two polarization states P^+ and P^- of a dynamically polarized deuteron target with the quantization axis perpendicular to the scattering plane. Following the Madison convention,¹⁹ we define the sign of the target polariza-

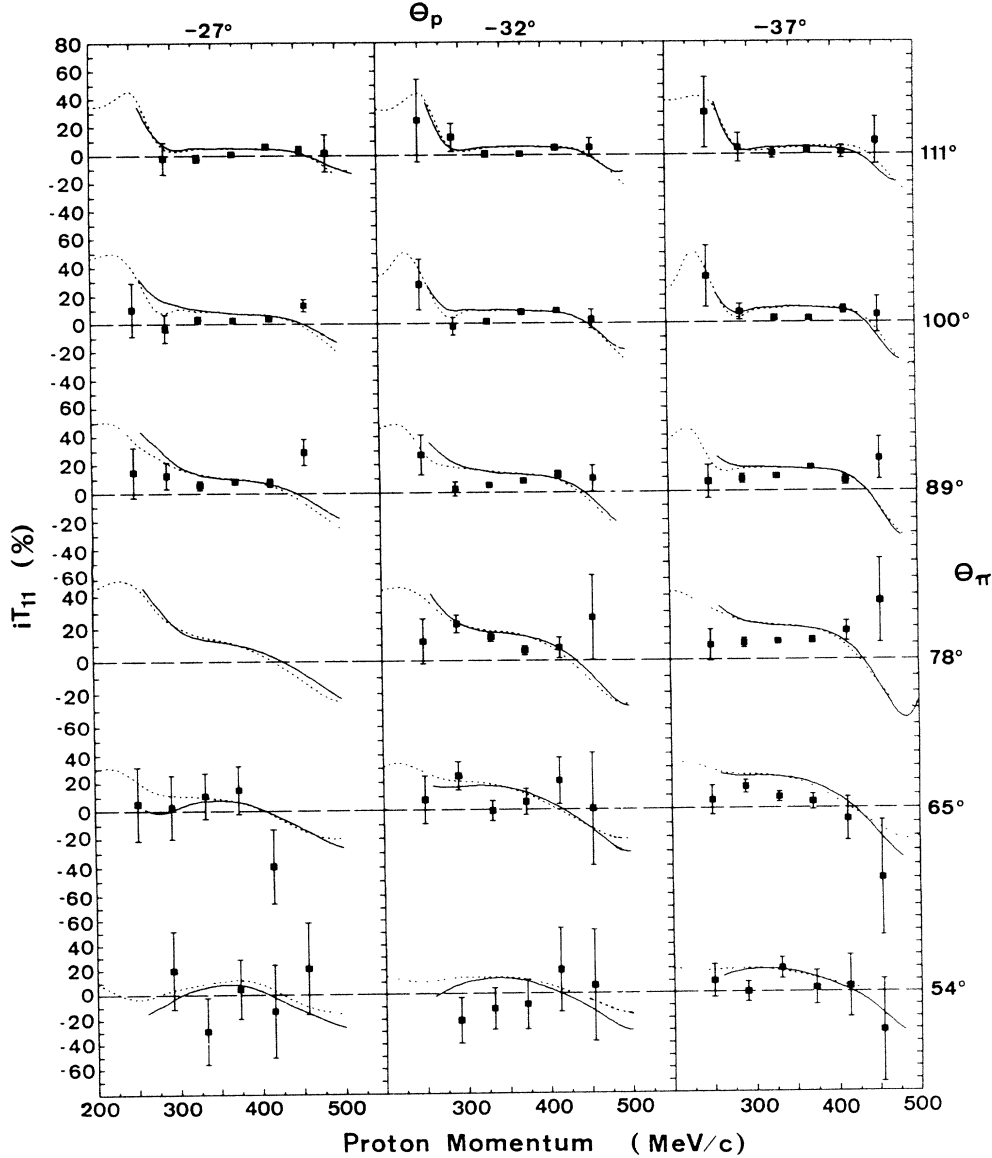


FIG. 1. Values of iT_{11} vs proton momentum for various pion-proton angle pairs at incident pion energy of 180 MeV. The solid and dashed lines are the results of the Faddeev calculations described in the text. Data are missing at one pair of angles but the calculation is shown.

tion to be positive for $\hat{n} = k_\pi \times k'_\pi$. The vector analyzing power is calculated from the expression

$$iT_{11} = \frac{1}{\sqrt{3}} \frac{\sigma^+ - \sigma^-}{\sigma^+ P^- + \sigma^- P^+ - \sigma^B (P^+ + P^-)},$$

where σ^+ and σ^- are the differential cross sections measured with target polarization P^+ and P^- and σ^B is the cross section measured with the background target. The cross sections are the threefold differential cross sections $d^3\sigma/d\Omega_\pi d\Omega_p dp$ as defined in the preceding paper. The detection system is also described there. The dynamically polarized target, used in this experiment, was discussed in detail in earlier publications.^{3,10} Here we discuss only those features which are specific to this experiment.

The principal differences from the cross section measurements were the effects of the background and the

magnetic field. Whenever polarized targets are used background events originate from nuclear reactions in the different target nuclei of the polarized target material. In πd reactions leading to two-body final states, like the pion elastic scattering or the pion absorption reaction, the TOF spectra obtained from the time differences of the two particles are narrow and can easily be separated from the TOF spectra of the background reactions which are broadened by Fermi motion in the nuclei. In the $\pi^+ d \rightarrow \pi^+ pn$ reaction, however, the foreground is also quite broad and the background must be measured carefully for every case where data are taken.

The target material of the polarized target consisted of deuterated butanol, i.e., C_4D_9OD . In earlier polarization experiments^{3,10} the target material was used either in the form of 1–2 mm diameter beads (for better cooling) which were immersed in liquid ^3He at 0.5 K, or as a

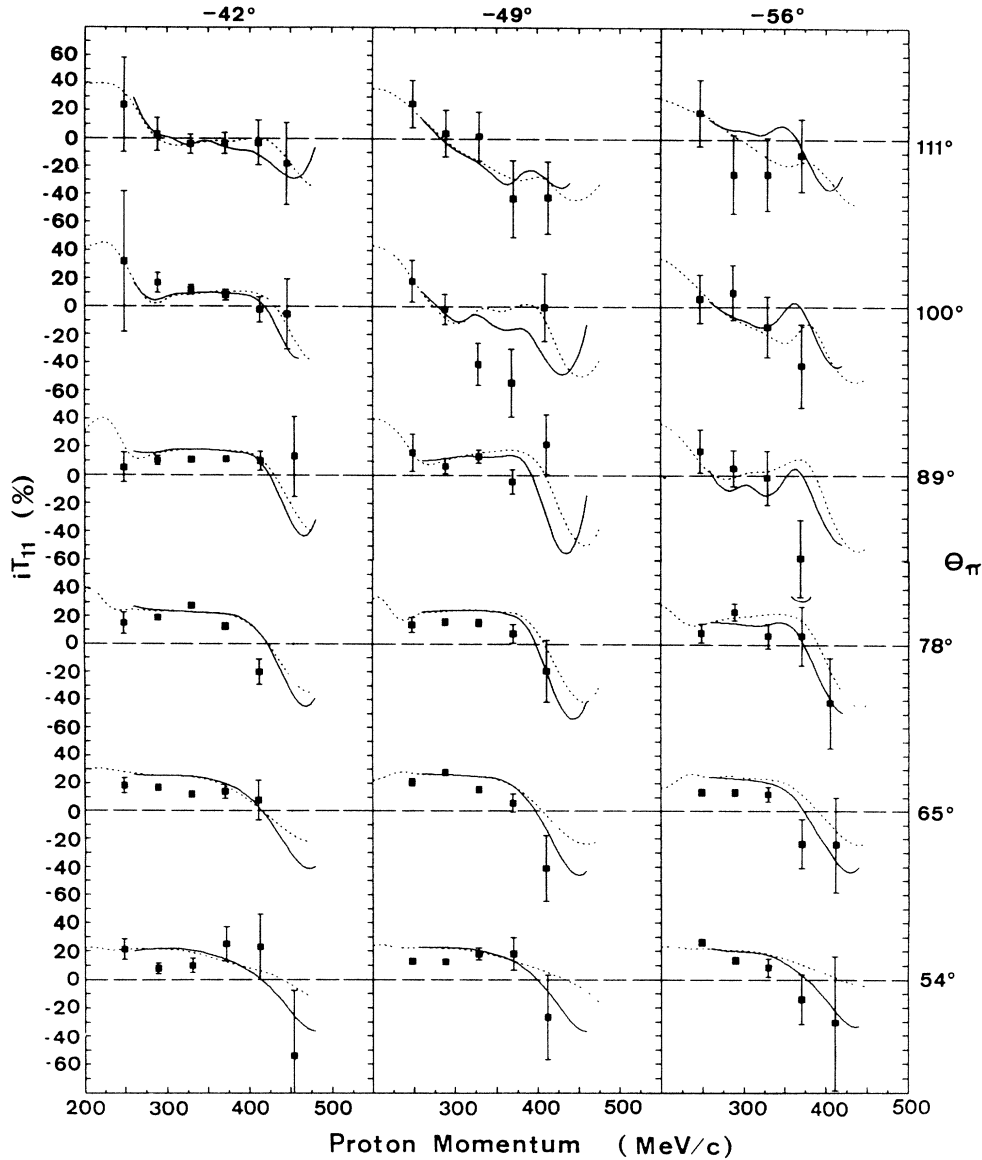


FIG. 2. The same as Fig. 1 at larger proton angles.

frozen slab, conduction cooled by the 0.1 mm thick brass walls of the target cell. This latter target form has the advantage that no ^3He is present in the target region; reactions in ^3He can produce unwanted (and difficult to measure) background events. Therefore in the present experiment where the subtraction of background events is crucial, we used the slab target configuration. The polarizations obtained were $P^+ = 0.175 \pm 0.04$ and $P^- = 0.20 \pm 0.04$.

A matching background target was made, consisting of layers of carbon and "dry ice" (solid CO_2) with the relative thickness chosen to be an appropriate " C_4O " target. The background target and an additional CH_2 target were mounted below the butanol target in the cryostat. Each target could be moved into the beam separately. The thickness of the background target was measured when it was made, but was checked by studying the background

subtractions of spectra from which events in the $\pi\pi$ breakup region were excluded. The relative thicknesses of the background and butanol targets were measured this way to within 5% and agreed with the original measured value. An error of 5% was assigned to the background target thickness in calculating the error of the vector analyzing power. The background from the carbon and oxygen nuclei in butanol and the brass target walls was similar to that from carbon in the CD_2 target used in the cross section measurement (see Fig. 3 of the preceding paper), but typically about 30% larger.

The 2.5 T magnetic field surrounding the polarized target acts like a momentum analyzer which distorts the pion and proton trajectories. In traversing the path from the target center to beyond the effects of the field, particles were deflected by an angle given approximately by $3200^\circ/p$ where p is the particle momentum in MeV/c .

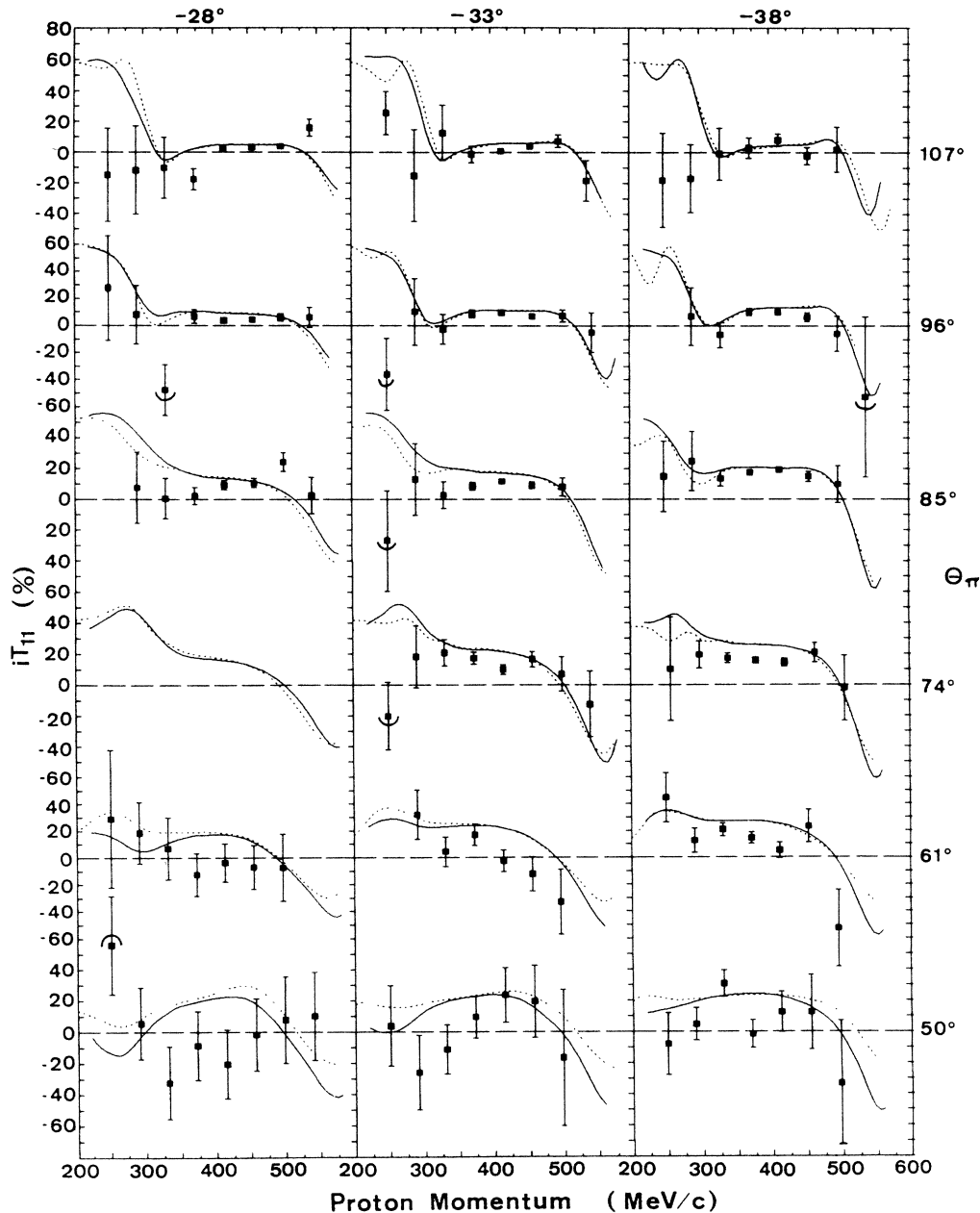


FIG. 3. Values of iT_{11} vs proton momentum for various pion-proton angle pairs at incident pion energy of 228 MeV. The solid and dashed lines are the results of the Faddeev calculations described in the text.

For a particular counter at a specific angle, the scattering angle with respect to the incident beam at the target center depends on the momentum of the detected particle. The trajectories and the mean times of flight of the particles (including the effects of energy losses in the target materials) were calculated with a ray tracing program. This program was checked by measuring the angles of protons from πp elastic scattering at fixed pion angles using the CH_2 target in the magnetic field. This reaction also allowed an absolute time calibration of the TOF spectra. The angular acceptance of the pion and proton counters was 5.8° and 4.4° , respectively.

Data were taken in approximately 2 h runs with the target polarization (+ or -) being changed in the sequence +, -, -, +, +, -, -, + followed by four background runs. This cycle was repeated until enough statistics were accumulated. This procedure of taking data was designed to cancel possible systematic shifts in efficiencies and calibrations. The target polarization was changed by altering the frequency of the polarizing microwave field (which induces hyperfine transitions in the target). The magnetic field remained constant.

The runs with the positively polarized, negatively polarized, and background targets were each summed and the

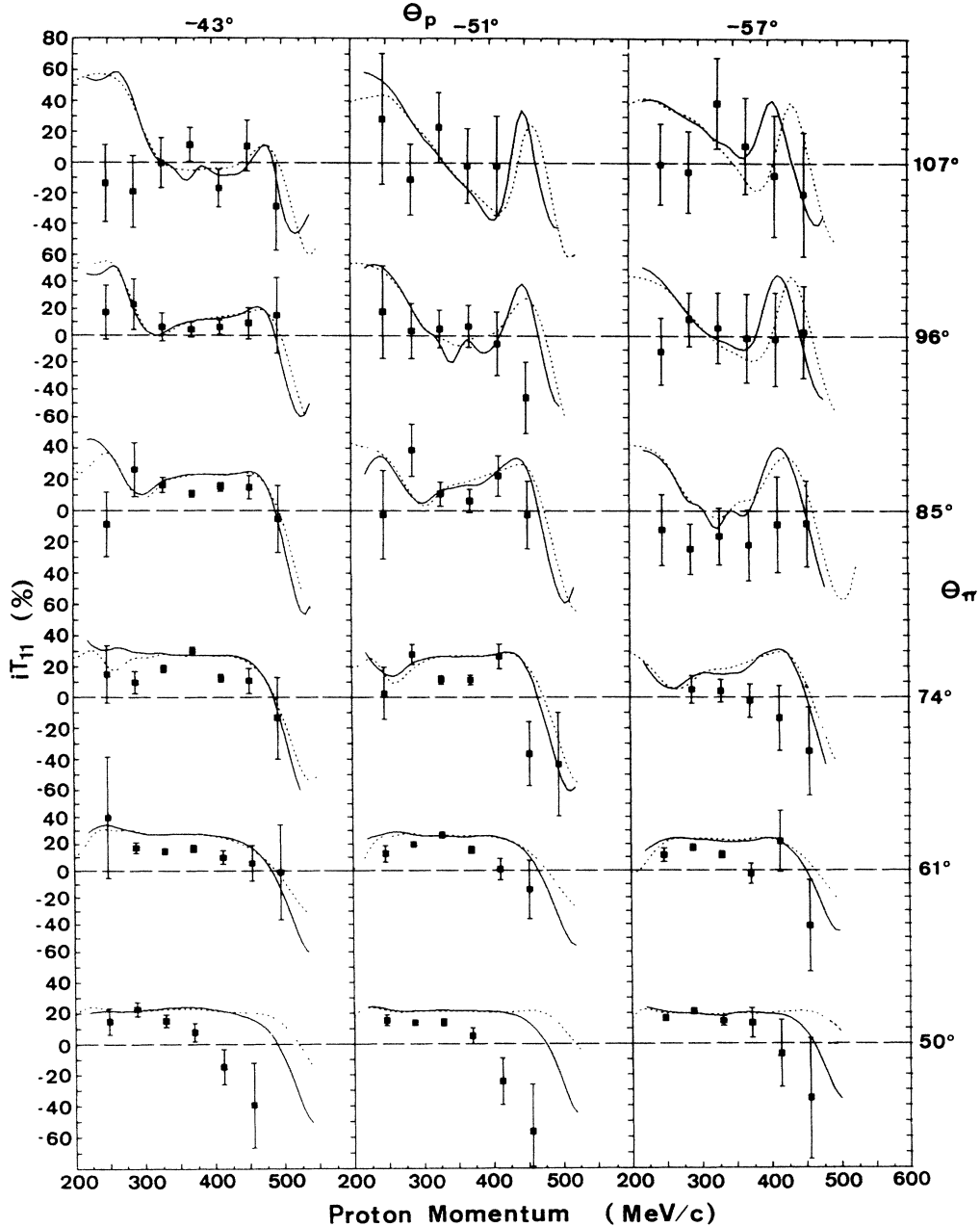


FIG. 4. The same as Fig. 3 at larger proton angles. Notice the “bumplike” structure in the theoretical predictions around 450 MeV/c in the upper-graphs. It is probably a manifestation of the Δ^{++} .

summed data analyzed. The vector analyzing power was calculated for 40 MeV/c bins in proton momentum for each pion-proton angle pair. As well as the statistical errors, the effect of the 5% uncertainty in the background target thickness is included in the error bars of the data points. To check for possible systematic effects during the data taking, a separate analysis was performed on each pair of positively and negatively polarized runs and a background run. These sets of results were then averaged and the statistical errors and the standard deviations of the means of each data point were calculated. Good agreement was found between the statistical errors and the

standard deviations of the means, showing an absence of significant systematic variations between different runs. Time varying systematic effects were also studied by performing the entire analysis with pairs of runs with equal target polarization (i.e., both positive or negative). The results of this analysis showed no significant deviations from zero, as expected.

III. RESULTS AND DISCUSSION

The experimental data are shown in Figs. 1–6. In the figure pairs 1 and 2, 3 and 4, and 5 and 6, the vector

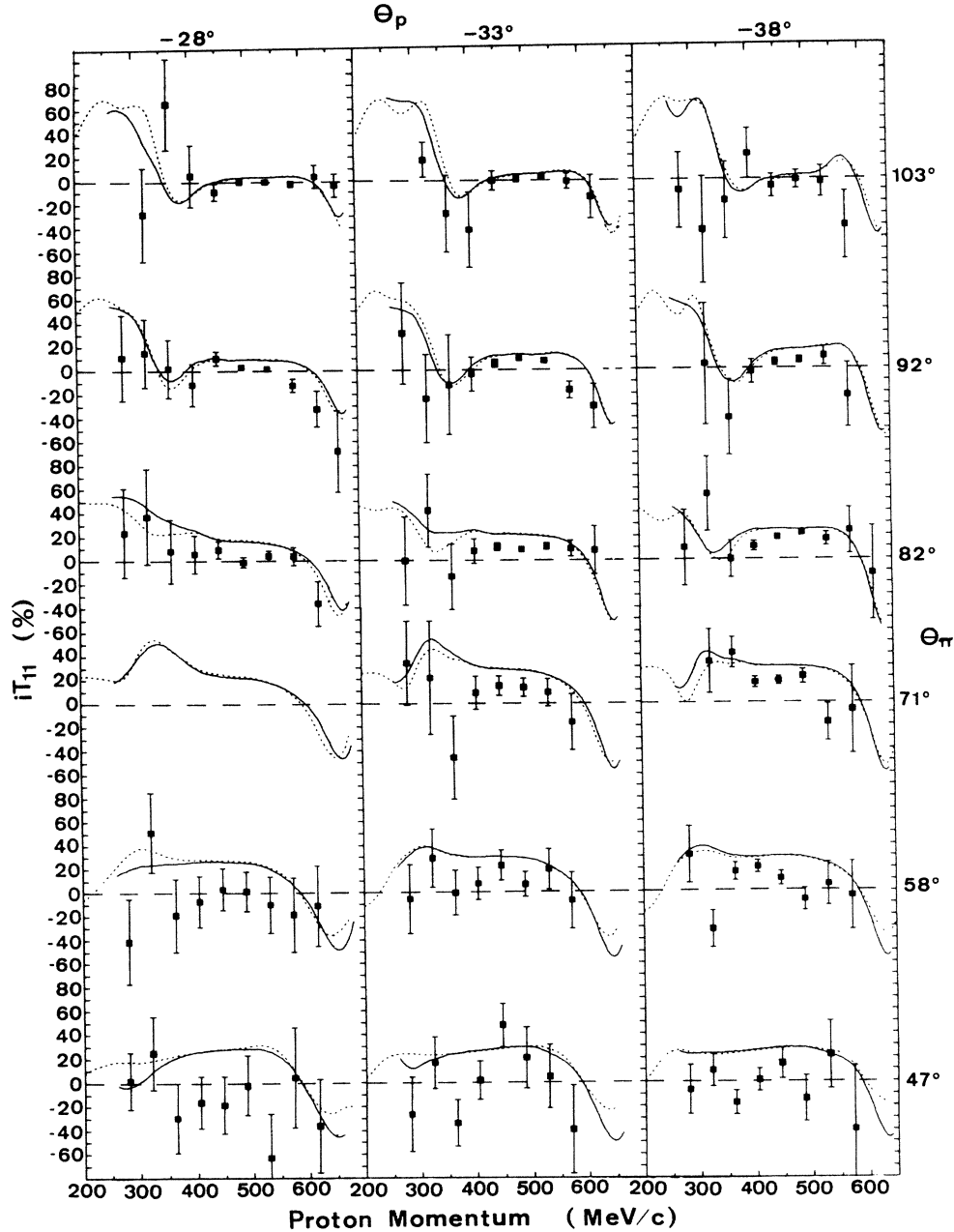


FIG. 5. Values of iT_{11} vs proton momentum for various pion-proton angle pairs at incident pion energy of 294 MeV. The solid and dashed lines are the results of the Faddeev calculations described in the text.

analyzing power iT_{11} is plotted as a function of the proton momentum for 35 pion-proton angle pairs at 180, 228, and 294 MeV incident pion energy (one pair is missing due to an intermittent failure of one coincidence unit in the electronic circuit). The graphs on the diagonal line from the upper left to the lower right corner correspond to nominal angle pairs of free πp kinematics. On both sides of this line the pion and proton angles increasingly depart from πp kinematics. Each data point in each of the 35 graphs corresponds to a pion and proton angle differing by a few degrees from the mean pion and proton angles quoted in the figure captions. This is due to the ef-

fect of the magnetic field of the polarized target on the particle trajectories.

In order to compare the data with the predictions from the Faddeev calculation described in the preceding publication, the vector analyzing power was calculated point by point, for the individual slightly varying angle pairs (solid line), and also for the mean pion-proton angle pairs (dashed line). No significant differences were found between these two kinds of calculations, and therefore the calculations for the mean angle pairs are also drawn in the figures in order to show the general trend of the theoretical predictions in those momentum regions where no data

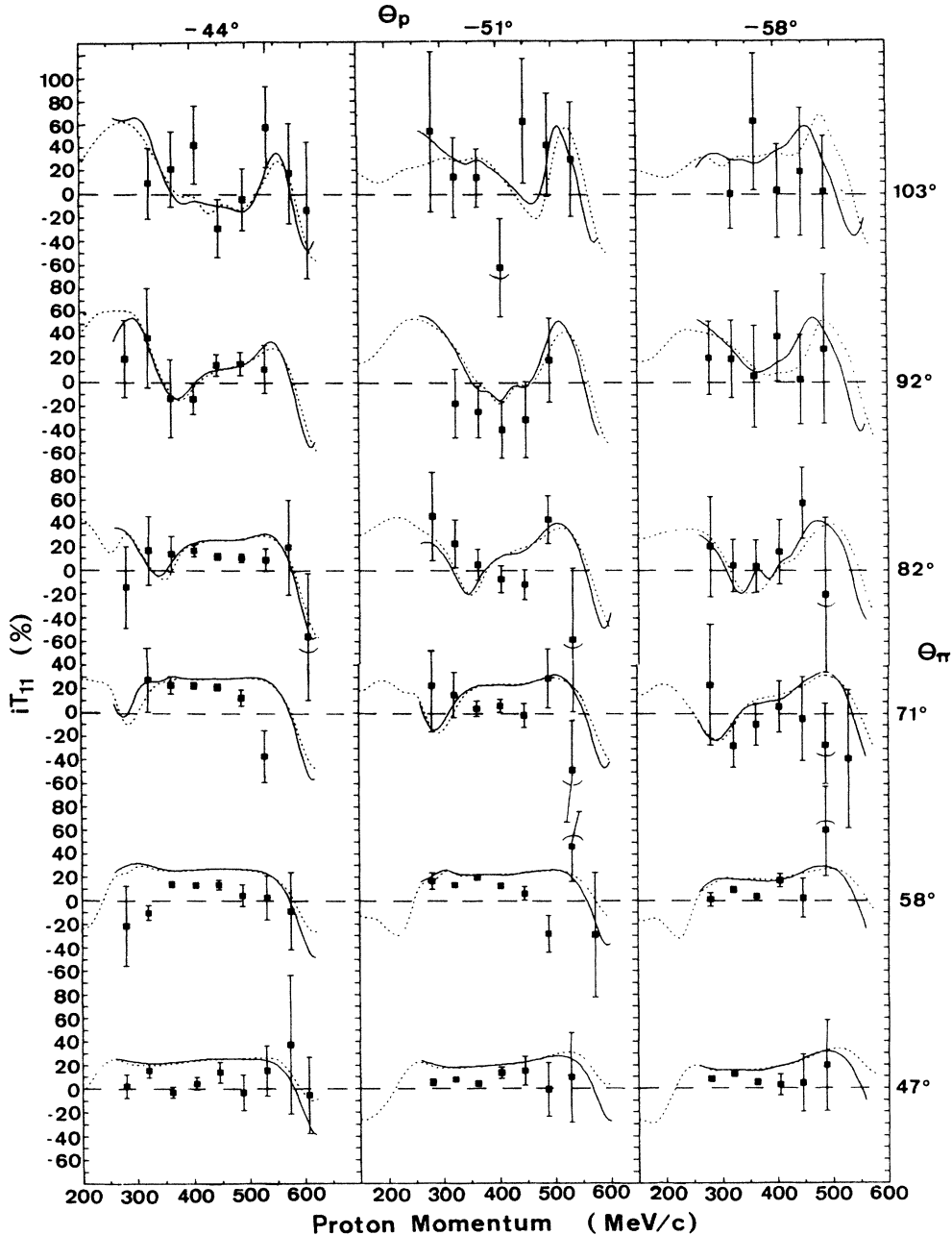


FIG. 6. The same as Fig. 5 at larger proton angles. Notice the “bumplike” structure in the theoretical predictions around 500 MeV/c in the upper-graphs. It is probably a manifestation of the Δ^{++} .

exist.

When comparing the bulk of the data with the theoretical predictions, one finds that the general trend of the data is well reproduced. Comparing theory and experiment in detail, three regions of proton momentum are of particular interest.

In the central momentum region (where the momentum of the final state neutron is small) iT_{11} is mostly positive and only slightly varying with momentum. In this region the data are very well reproduced by the theory. It is interesting to compare iT_{11} at exactly the quasifree πp

kinematics with the polarization, P , of the free πp scattering, as calculated from πp phase shifts.²⁰ We have used the relationship $iT_{11} = P/\sqrt{3}$ for this comparison, neglecting effects due to the D state of the deuteron. The results are shown in Fig. 7. The momentum acceptance of each of these data points is 40 MeV/c. The dotted line represents the πp polarization. The solid lines are the results of the Faddeev calculation. As one can see there is very good agreement between the quasifree and the free πp data at all energies. Excellent agreement with the theoretical prediction occurs at 180 and 228 MeV. At 294

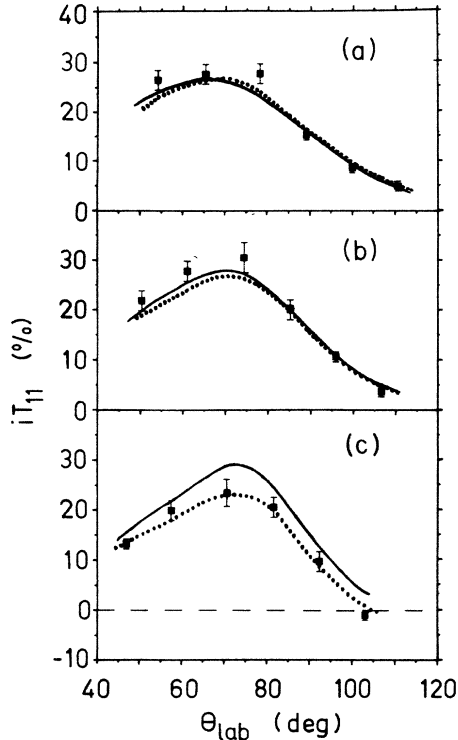


FIG. 7. Values of iT_{11} at pion-proton angles and momenta corresponding to quasifree πp scattering. The incident pion energies are the following: (a) 180 MeV, (b) 228 MeV, and (c) 294 MeV. The dotted curves are predictions of P for free $\pi\pi$ scattering calculated from πp phase shifts (Ref. 20). The solid lines are the results of the Faddeev calculations described in the text.

MeV the theory predicts iT_{11} somewhat larger than the data.

In the high momentum region the data display a rather rapid change of iT_{11} from positive to negative values. Also this trend is predicted by the theoretical calculations. It is interesting to observe that the crossover of iT_{11} varies only little within all 35 graphs of one particular pion bombarding energy. It occurs almost invariably around 400 MeV/c for the data at 180 MeV, around 500 MeV/c for the data at 228 MeV, and around 600 MeV/c for those at 294 MeV.

In the low momentum region the theoretical calculations are extremely sensitive to the proton-neutron final state interaction (FSI), as has been observed in a test calculation where the FSI was turned off. In Fig. 8 two calculations for the cross sections and the polarization observables iT_{11} and T_{20} are shown, one including the FSI (solid lines) and one excluding the pn FSI (dashed lines). As one can see, the observable iT_{11} is most sensitive to the FSI. More precise data will be needed to test the theoretical predictions in this region. In addition it will be valuable to measure T_{20} for this reaction as soon as tensor polarized targets are available. According to the theoretical calculation, sizable analyzing powers, T_{20} , are to be expected in some regions of the proton momentum.

The πd breakup reaction is closely related to the coupled inelastic pp scattering reactions. It is interesting to compare the present results for the $\pi d \rightarrow \pi pn$ reaction

with those of the asymmetry, A_y , for the $\bar{p}p \rightarrow \pi pn$ reaction. This reaction was measured in a kinematically complete experiment at $T_p = 800$ MeV (corresponding to $T_\pi = 256$ MeV for the same center of mass energy).¹¹ The momentum dependence of the asymmetry A_y was determined between 500 and 1000 MeV/c for 12 pion proton angle pairs. Although the mechanism for this reaction [the dominant production of the Δ^{++} (Ref. 21)] is quite different from the one of the pion deuteron breakup reaction, the asymmetry, A_y , shows similar features in comparable momentum regions as the vector analyzing power iT_{11} . For a number of angle pairs A_y is positive (applying the same sign convention for the positive polarization axis as was used in this experiment; $\hat{n} = k_\pi \times k'_\pi$) and almost constant in the central momentum region. At higher momenta it almost linearly changes to large negative A_y values. Dubach *et al.*²² have calculated the analyzing power using the unitary model of Kloeet and Silbar.²³ This model, which as mentioned in the preceding paper is also based on the AAY relativistic Faddeev equations, includes all spin complications, and preserves two- and three-body unitarity. Dubach *et al.* were able to correctly predict the analyzing power for some pion-proton angle pairs but fail for others.

More recently, several Wolfenstein parameters have been measured for the spin transfer reaction $\bar{p}p \rightarrow \bar{p}\pi^+n$ at 650, 733, and 800 MeV over the proton momentum range 700–1200 MeV/c.²⁴ These data represent a considerable increase in the knowledge of the spin dependence of the $pp \rightarrow p\pi^+n$ reaction. At present only the unified, unitary model by Dubach, Kloeet, and Silbar²⁵ has been applied to this reaction. In spite of the simplified physics input used in the calculation (including only the P_{33} and P_{11} pion-nucleon partial waves and not including the various short-range NN interactions) the general trend of the polarization data is rather well reproduced.

IV. SUMMARY

The present study was carried out in order to present the theoretical community with extensive data on the πd breakup reactions, which can be used to put a more stringent test on the various relativistic three-body theories that have been proposed in recent years. This is particularly important with regard to the “classical” relativistic three-body theory of Aaron, Amado, and Young²⁶ (AAY), which has been strongly criticized by the proponents of the “new” NN- π NN theory,^{27,28} arguing that the AAY theory does not make any special effort to distinguish the double role of the pion as an independent particle and at the same time as the mediator of the nucleon-nucleon force.

The ultimate test of a theory is its comparison with experiment, and therefore it is significant that the “classical” AAY theory after having been able to describe successfully the elastic πd reaction including differential cross section, vector analyzing power, iT_{11} , and tensor polarization, t_{20} (from Ref. 29), can describe also the πd -

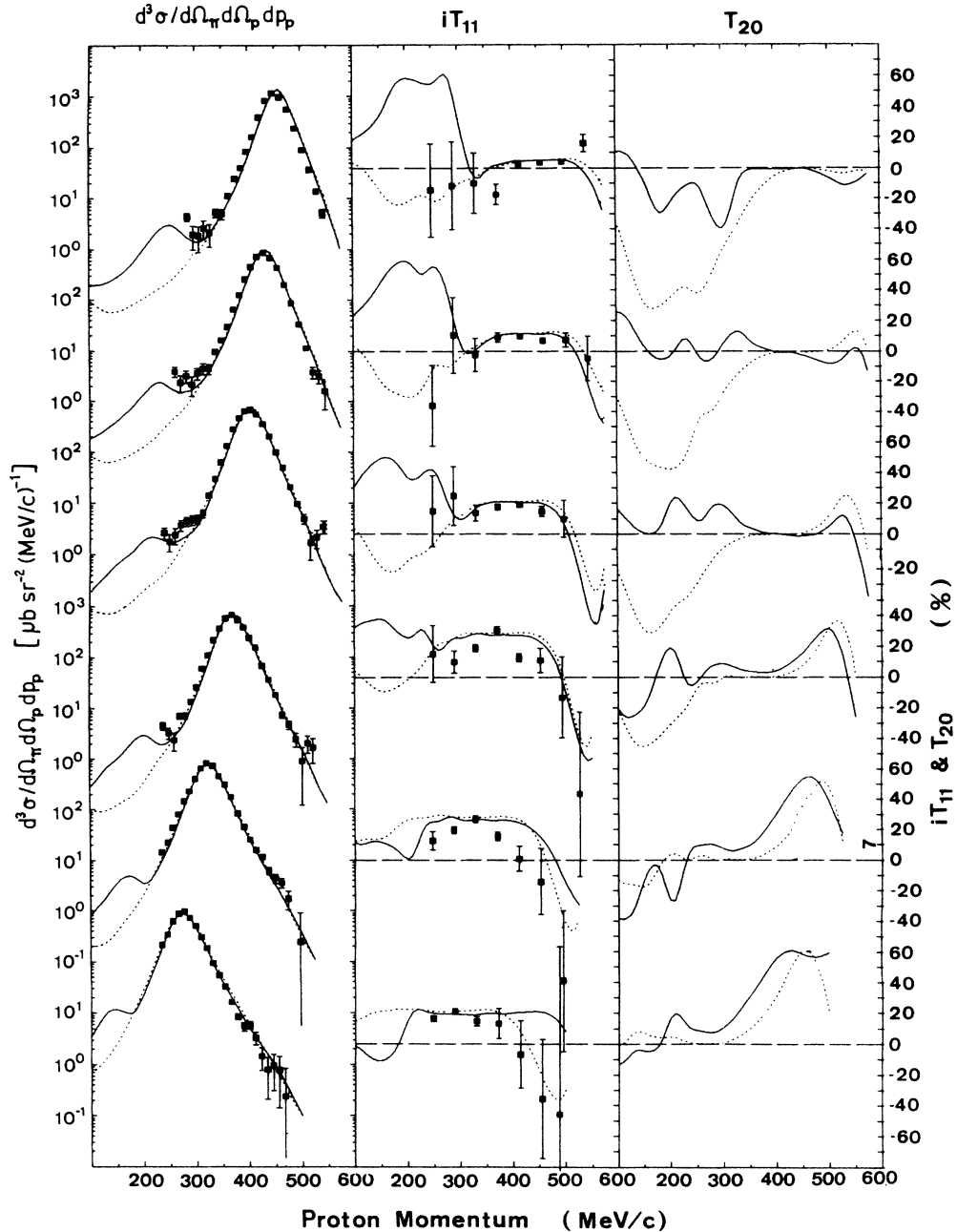


FIG. 8. Effect of the pn final state interaction on the differential cross section, and the polarization observables iT_{11} and T_{20} at $T_\pi = 228$ MeV. The solid lines represent the full Faddeev calculation and the dashed lines correspond to a calculation where the final state interaction was excluded. The pion-proton angle pairs are from top to bottom (107,28), (96,33), (85,38), (74,43), (61,51), and (50,57) degrees. The cross section data are from the preceding and the iT_{11} data are from the present publication.

breakup differential cross section, and vector analyzing power, iT_{11} .

The $NN-\pi NN$ theory, as mentioned in our preceding paper, already has problems in trying to describe the πd -elastic polarization observables. Thus, we see the results of our theoretical and experimental studies as containing a vindication of the "classical" AAY theory, while the burden of the confrontation with experiment is now upon the proponents of the $NN-\pi NN$ theory.

ACKNOWLEDGMENTS

The help of R. Olszewski during the setting up and data taking phase of this experiment was greatly appreciated. This work would have been impossible without the generous help and the considerable skills of the staff of SIN. This work was supported by the Bundesministerium für Forschung und Technologie of the Federal Republic of Germany.

*Permanent address: Escuela Superior de Física y Matemáticas, Instituto Politécnico Nacional, México 14, D.F., Mexico.

†Present address: University of Regina, Regina, Saskatchewan, Canada S4S 0A2.

‡Present address: TRIUMF, Vancouver, British Columbia, Canada V6T 2A3.

¹A. Yokosawa, *Phys. Rep.* **65**, 53 (1980); H. Spinka, Los Alamos National Laboratory Report LA 8775-C, 1981 (unpublished).

²R. R. Silbar, *Comments Nucl. Part. Phys.* **12**, 177 (1984).

³G. R. Smith *et al.*, *Phys. Rev. C* **29**, 2206 (1984).

⁴J. Ulbricht *et al.*, *Phys. Rev. Lett.* **48**, 311 (1982); W. Gruebler *et al.*, *ibid.* **49**, 444 (1982); R. J. Holt *et al.*, *ibid.* **47**, 472 (1981); E. Ungricht *et al.*, *ibid.* **52**, 333 (1984).

⁵H. Garcilazo, *Phys. Rev. Lett.* **53**, 652 (1984); E. Ungricht *et al.*, *Phys. Rev. C* **31**, 934 (1985).

⁶I. R. Afnan and R. S. McLeod, *Phys. Rev. C* **31**, 1821 (1985).

⁷J. A. Niskanen, *Phys. Lett.* **141B**, 301 (1984); A. S. Rinat and Y. Starkand, *Nucl. Phys.* **A397**, 381 (1983); J. L. Perrot, Ph.D. thesis, University of Lyon Report LYCEN 8409, 1984.

⁸M. P. Locher and A. Svarč, *J. Phys. G* **11**, 183 (1985).

⁹D. V. Bugg, *Nucl. Phys.* **A437**, 534 (1985).

¹⁰G. R. Smith *et al.*, *Phys. Rev. C* **30**, 980 (1984).

¹¹A. D. Hancock *et al.*, *Phys. Rev. C* **27**, 2742 (1983).

¹²T. S. Bhatia *et al.*, Los Alamos National Laboratory Report LA-UR-83-215, 1983.

¹³R. Shypit *et al.*, *Phys. Lett.* **124B**, 314 (1983).

¹⁴I. P. Auer *et al.*, *Phys. Rev. Lett.* **51**, 1411 (1983).

¹⁵E. Aprile-Giboni *et al.*, University of Geneva report, 1984.

¹⁶A. König and P. Kroll, *Nucl. Phys.* **A356**, 45 (1981); W. M. Kloet and R. R. Silbar, *ibid.* **A364**, 346 (1981).

¹⁷W. Jauch, A. König, and P. Kroll, University of Wuppertal Report WU B84-7, 1984.

¹⁸E. L. Mathie *et al.*, *Phys. Lett.* **154B**, 28 (1985).

¹⁹*Proceedings of the Third International Symposium on Polarization Phenomena in Nuclear Reactions, Madison, 1970*, edited by H. H. Barschall and W. Haeberli (University of Wisconsin, Madison, 1971).

²⁰R. A. Arndt and L. D. Roper, Virginia Polytechnic Institute and State University, Internal Report CAPS-80-3, 1982.

²¹J. Hudomalj-Gabitzsch *et al.*, *Phys. Rev. C* **18**, 2666 (1978).

²²J. Dubach *et al.*, *Phys. Lett.* **106B**, 29 (1981).

²³W. Kloet and R. Silbar, *Nucl. Phys.* **A338**, 231 (1980); **A338**, 317 (1980).

²⁴C. L. Hollas *et al.*, *Phys. Rev. Lett.* **55**, 29 (1985).

²⁵J. Dubach, W. M. Kloet, A. Cass, and R. R. Silbar, *Phys. Lett.* **106B**, 28 (1981); J. Dubach, W. M. Kloet, and R. R. Silbar, *J. Phys. G* **8**, 475 (1982).

²⁶R. Aaron, R. D. Amado, and J. E. Young, *Phys. Rev.* **174**, 2022 (1968).

²⁷Y. Avishai and T. Mitzutani, *Nucl. Phys.* **A326**, 352 (1979); **A338**, 377 (1980); **A352**, 399 (1981); *Phys. Rev. C* **27**, 312 (1983).

²⁸B. Blankleider and I. R. Afnan, *Phys. Rev. C* **24**, 1572 (1981).

²⁹E. Ungricht *et al.*, *Phys. Rev. C* **31**, 934 (1985).